REFERENCES

[1] H. G. Musmann, P. Pirsch, and H. J. Grallert, "Advances in picture coding," *Proc. IEEE*, vol. 73, pp. 523–548, Apr. 1985.

[2] CCITT, Recommend. H. 261, "Video codec for audiovisual services at *P*x64 kbit/s," Geneva, Switzerland, Aug. 1990.

[3] D. J. LeGall, "MPEG: A video compression standard for multimedia applications," *Commun. ACM*, vol. 34, pp. 47–58, Apr. 1991.

[4] G. Giunta, T. R. Reed, and M. Kunt, "Image sequence coding using oriented edges," *Signal Process.: Image Commun.*, vol. 2, no. 4, pp. 429–440, 1990.

[5] R. Aravind *et al.*, "Image and video coding standards," *AT&T Tech. J.*, vol. 72, pp. 67–88, Jan./Feb. 1993.

[6] C. Morimoto, P. Burlina, and R. Chellappa, "Video coding using hybrid motion compensation," in *Proc. Int. Conf. Image Processing*, Oct. 26–29, 1997, vol. 1, pp. 89–92.

[7] J. K. Aggarwal and N. Nandhakumar, "On the computation of motion from sequences of images—A review," *Proc. IEEE*, vol. 76, pp. 917–935, 1988.

[8] J. H. Moon and J. K. Kim, "On the accuracy and convergence of 2D motion models using minimum MSE motion estimation," *Signal Process.: Image Commun.*, vol. 6, pp. 319–333, 1994.

[9] R. Rajagopalan, M. T. Orchard, and R. D. Brandt, "Motion field modeling for video sequences," *IEEE Trans. Image Processing*, vol. 6, pp. 1503–1515, Nov. 1997.

[10] F. Moscheni, F. Dufaux, and M. Kunt, "A new two-stage global/local motion estimation based on a background/foreground segmentation," in *Proc. Int. Conf. on Acoustics, Speech, and Signal Processing*, May 9–12, 1995, vol. 4, pp. 2261–2264.

[11] C. K. Cheong and K. Aizawa, "Structural motion segmentation based on probabilistic clustering," in *Proc. Int. Conf. Image Processing*, Sept. 16-19, 1996, pp. 505–508.

[12] K. Zhang, M. Bober, and J. Kittler, "Image sequence coding using multiple-level segmentation and affine motion estimation," *IEEE J. Select. Areas Commun.*, vol. 15, pp. 1704–1713, Dec. 1997.

[13] M. M. Chang, A. M. Tekalp, and M. I. Sezan, "Simultaneous motion estimation and segmentation," *IEEE Trans. Image Processing*, vol. 6, pp. 1326–1333, Sept. 1997.

[14] C. Cafforio, E. DiSciascio, and C. Guaragnella, "Motion estimation and modeling for video sequences," in *Proc. IX Eur. Signal Processing Conf., EUSIPCO-98*, Rhodes, Greece, Sept. 8–11, 1998, pp. 1557–1560.

[15] G. J. Keesman, "Motion estimation based on a motion model incorporating translation, rotation and zoom," in *Signal Process. IV: Theory Applicat.*, vol. 1, pp. 31–34, 1988.

[16] M. Hoetter, "Differential estimation of the global motion parameters zoom and pan," *Signal Process.*, vol. 16, pp. 249–265, 1989.

[17] S. F. Wu and J. Kittler, "A differential method for simultaneous estimation of rotation, change of scale and translation," *Signal Process.: Image Commun.*, vol. 2, pp. 69–80, 1990.

[18] Z. Eisips and D. Malah, "Global motion estimation for image sequence coding applications," in *Proc. 17th Conv. Electrical and Electronics Engineering*, Israel, 1991, pp. 186–189.

[19] Y. T. Tse and R. L. Baker, "Global zoom/pan estimation and compensation for video compression," in *Proc. Int. Conf. Acoustics, Speech, Signal Processing*, vol. 4, pp. 2725–2728, 1991.

[20] A. Amitay and D. Malah, "Global-motion estimation in image sequences of 3-D scenes for coding applications," *Signal Process.: Image Commun.*, vol. 6, pp. 507–520, 1995.

[21] W. Chen, G. B. Giannakis, and N. Nandhakumar, "Spatiotemporal approach for time-varying global image motion estimation," *IEEE Trans. Image Processing*, vol. 5, pp. 1448–1461, Oct. 1996.

[22] M. Irani, B. Rousso, and S. Peleg, "Recovery of ego-motion using region alignment," *IEEE Trans. Pattern Anal. Machine Intell.*, vol. 19, pp. 268–272, Mar. 1997.

[23] C. Silva and J. Santos-Victor, "Robust egomotion estimation from the normal flow using search subspaces," *IEEE Trans. Pattern Anal. Machine Intell.*, vol. 19, pp. 1026–1034, Sept. 1997.

[24] G. Giunta, "Fast estimators of time delay and Doppler stretch based on discrete-time methods," *IEEE Trans. Signal Processing*, vol. 46, pp. 1785–1797, July 1998.

[25] G. Giunta and U. Mascia, "An optimal estimator of camera motion by a nonstationary image model," in *Proc. 5th Int. Workshop on Time-Varying Image Processing and Moving Object Recognition 4*, Florence, Italy, Sept. 5–6, 1996, pp. 57–62.

[26] Y. S. Jehng, L. G. Chen, and T. D. Chiueh, "An efficient and simple VLSI tree architecture for motion estimation algorithms," *IEEE Trans. Signal Processing*, vol. 41, pp. 889–900, Feb. 1993.

[27] C. Cafforio and F. Rocca, "Methods for measuring small displacements of television images," *IEEE Trans. Inform. Theory*, vol. IT-22, pp. 573–579, Sept. 1976.

[28] G. Giunta, "Fine estimators of 2D parameters and application to spatial shift estimation," *IEEE Trans. Signal Processing*, to be published.

[29] H. M. Kim and B. Kosko, "Neural fuzzy motion estimation and compensation," *IEEE Trans. Signal Processing*, vol. 45, pp. 2315–2532, Oct. 1997.

Regularized Total Least Squares Approach for Nonconvolutional Linear Inverse Problems

Wenwu Zhu, Yao Wang, Nikolas P. Galatsanos, and Jun Zhang

***Abstract*— In this correspondence, a solution is developed for the regularized total least squares (RTLS) estimate in linear inverse problems where the linear operator is nonconvolutional. Our approach is based on a Rayleigh quotient (RQ) formulation of the TLS problem, and we accomplish regularization by modifying the RQ function to enforce a smooth solution. A conjugate gradient algorithm is used to minimize the modified RQ function. As an example, the proposed approach has been applied to the perturbation equation encountered in optical tomography. Simulation results show that this method provides more stable and accurate solutions than the regularized least squares and a previously reported total least squares approach, also based on the RQ formulation.**

***Index Terms*— Image reconstruction, image recovery, image restoration, inverse problems, optical tomography, regularization, tomographic imaging.**

I. INTRODUCTION

Many important image processing and medical imaging problems, such as restoration, reconstruction, motion estimation, and segmentation, can be formulated as inverse problems where the original image or data is corrupted by noise. When we reconstruct the original image or data, mathematically it is required to obtain the solution of a linear equation

$$\mathbf{H}\mathbf{x} = \mathbf{y} \tag{1}$$

where $\mathbf{x}$ is an $n \times 1$ vector of the original image or data, $\mathbf{y}$ is an $m \times 1$ vector of the corrupted date by noise in the measurement,

Manuscript received March 26, 1998; revised March 31, 1999. This work was supported in part by the National Institutes of Health under Grants RO1-CA59955 and R01-CA66184. The associate editor coordinating the review of this manuscript and approving it for publication was Prof. W. Clem Karl.

W. Zhu is with Bell Laboratories, Lucent Technologies, Murray Hill, NJ 07974-0636 USA.

Y. Wang is with the Department of Electrical Engineering, Polytechnic University, Brooklyn, NY 11201 USA.

N. P. Galatsanos is with the Department of Electrical and Computer Engineering, Illinois Institute of Technology, Chicago, IL 60616 USA.

J. Zhang is with the Department of Electrical Engineering and Computer Science, University of Wisconsin-Milwaukee, Milwaukee, WI 53201 USA.

Publisher Item Identifier S 1057-7149(99)08757-6.

and $\mathbf{H}$ is a linear operator which is an $m \times n$ matrix. In most cases, (1) is ill-posed. For some applications, such as tomographic imaging, the inverse problem is also under-determined due to the fact that the number of detector readings m is smaller than the number of unknowns n. Even if $m \geq n$, the matrix $\mathbf{H}$ could be rank deficient, which also leads to an under-determined system. When only the data $\mathbf{y}$ are corrupted by noise, the regularized least squares (RLS) approach is usually used to reduce the sensitivity to the noise in the data $\mathbf{y}$ [1]. With this approach, measurement data and *a priori* knowledge about the original image (data) are used in a complementary way.

In some cases, the linear operator $\mathbf{H}$ may be also subject to errors or noise. For example, in many tomographic imaging applications this results from the approximations used in deriving the linear model and the numerical errors in computing $\mathbf{H}$. In these cases, a total least-squares (TLS) solution of (1) is optimal in the sense that errors in both the operator and measurement data are minimized [2]. Justice *et al.* applied the TLS approach to geophysical diffraction tomography [3]. Li *et al.* [4] employed the TLS method in phased array imaging where noise in $\mathbf{H}$ and $\mathbf{y}$ are assumed independent. The TLS solution in the above examples is obtained using singular value decomposition (SVD). However, this may run into computational difficulties for large-scale systems since the classical SVD computation requires $\sim 12n^3$ multiplications [5], where n is the number of the unknowns [6]. As an alternative, we proposed a Rayleigh quotient form TLS (RQF-TLS) approach in [7]. It reaches the TLS solution by iteratively minimizing a Rayleigh quotient function (QRF). Because it needs $\sim n^2$ multiplications per iteration, and for large n, usually less than n iterations are required, this approach may be more suitable for large scale problems.

In general, the imaging operator $\mathbf{H}$ is ill-conditioned. To deal with this problem, regularization is often used. In [8], this is accomplished by truncating the singular values in SVD [8]. In [9] and [10], the authors apply the principle of Tikhonov regularization in the TLS framework. There $\mathbf{H}$ is a *convolutional* operator, which corresponds to the point spread function (PSF), and the noise in $\mathbf{H}$ and the data are colored and independent. In [9], signals were assumed stationary and, using the diagonalization properties of the discrete Fourier transform (DFT), the problem was cast in a scalar form in the DFT domain which allows efficient computation iteratively even for large images. In this work, we focus on the problem when $\mathbf{H}$ is *nonconvolutional* where a DFT formulation cannot be used. Specifically, to improve the stability of the RQF-TLS solution, regularization is incorporated into the RQF-TLS formulation. To minimize the modified RQF, a conjugate gradient (CG) method [11], [12] is employed, although for small size problems, a direct SVD approach can also be used. In the remainder of this work, this method is referred to as RQF-RTLS.

The rest of this correspondence is organized as follows. In Section II, the RQF-TLS approach is briefly reviewed and the regularized total least-squares formulation based on Rayleigh quotient is described. Section III presents simulation results. Finally, Section IV provides a summary and conclusions.

II. Regularized Total Least Squares Solution Based on Rayleigh Quotient Formulation

The RQF-TLS solution is expressed by [7]

$$\text{minimize}\left\{F(\mathbf{q}) = \frac{\mathbf{q}^T\mathbf{A}^T\mathbf{A}\mathbf{q}}{\mathbf{q}^T\mathbf{q}}\right\} \tag{2}$$

where $F(\mathbf{q})$ is called the Rayleigh quotient

$$\mathbf{A} = [\mathbf{H} \mid \mathbf{y}] \tag{3}$$

and

$$\mathbf{q} = \begin{pmatrix} \mathbf{x} \\ -1 \end{pmatrix}.$$

The solution of (2) is equal to the eigenvector $\mathbf{q}$ associated with the smallest eigenvalue of $\mathbf{A}^T\mathbf{A}$.

The RQF-TLS solution is in general ill-posed, i.e., the solution is sensitive to noise, and is underdetermined when the matrix $\mathbf{H}$ is rank deficient. In this work, we use regularization to stabilize the solution of the RQF-TLS problem. For the LS problem (which minimizes the perturbation in the data vector $\mathbf{y}$), a penalty term which forces the solution vector $\mathbf{x}$ to be smooth or have finite energy is usually imposed to overcome the ill-conditioning of the matrix $\mathbf{H}$. The penalty term normally has the form of $\|Q\mathbf{x}\|^2$, where $\mathbf{Q}$ is the desired regularization operator, which can be the first-order or second-order difference of the original image or data. In general if the original image or data is discontinuous, the first-order derivative is used. If the original image or data is smooth, usually the second-order derivative is used.

For the RQF-TLS, we can similarly add a penalty term to enforce the finite energy and/or smoothness constraint. The trick here is to add the penalty term in such a way so that the minimizing function still has the RQ form of (2). Motivated by this consideration, we propose to minimize the following modified RQF:

$$\begin{aligned} E(\mathbf{q}) &= \frac{\mathbf{q}^T\mathbf{A}^T\mathbf{A}\mathbf{q}}{\mathbf{q}^T\mathbf{q}} + \lambda\frac{\|\mathbf{Q}\mathbf{x}\|^2 + 1}{\mathbf{q}^T\mathbf{q}} \\ &= \frac{\mathbf{q}^T[\mathbf{A}^T\mathbf{A} + \lambda\mathbf{C}^T\mathbf{C}]\mathbf{q}}{\mathbf{q}^T\mathbf{q}} = \frac{\mathbf{q}^T\mathbf{B}\mathbf{q}}{\mathbf{q}^T\mathbf{q}} \end{aligned} \tag{4}$$

where

$$\mathbf{C} = \begin{pmatrix} \mathbf{Q} & 0 \\ 0 & 1 \end{pmatrix}$$

and

$$\mathbf{B} = \mathbf{A}^T\mathbf{A} + \lambda\mathbf{C}^T\mathbf{C}.$$

Obviously, (4) is still in the RQ form. In this study, we choose $\mathbf{Q}$ as a discrete approximation of the 2-D Laplacian operator in order to impose smoothness on the solution. The regularization parameter λ was determined using a trial-and-error process in our simulations which is briefly described in the next section.

Minimizing (4) is equivalent to determining the eigenvector associated with the smallest eigenvalue of $\mathbf{B}$. Therefore, the regularized TLS solution can be directly obtained by a SVD method applied to $\mathbf{B}$. We choose to use the CG method, as with the previously reported RQF-TLS approach [7], which is computationally more manageable than the direct SVD method for large size problems (e.g., $n > 1000$). This is because the CG method usually requires less than n iterations to converge and it takes $\sim n^2$ flops per iteration [11]. Hence, the CG method usually requires less than $\sim n^3$ flops. On the other hand, the SVD method requires $\sim 12n^3$ flops [5, Ch. 12]. When the $\mathbf{H}$ matrix is sparse, which is true for most tomographic problems, the computational saving from using a CG method will be more significant than a direct SVD approach [12].

III. Simulation Results

As an example, the proposed RQF-RTLS approach has been applied to the perturbation equation encountered in optical tomography [14], [15]. We attempted the reconstruction of several test media using numerically simulated data. Each test medium was infinite and homogeneous except at the location of an embedded rod. A total of 16 sources and 16 detectors were evenly spaced around

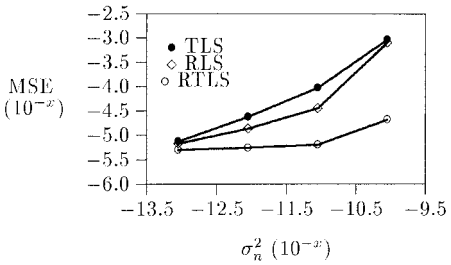

Fig. 1. MSE's of reconstructed images of the off-center case obtained by different methods under different σ_n^2 for a given $\sigma_h^2 = 8.99E{-}12$. Both axes are represented in terms of exponents.

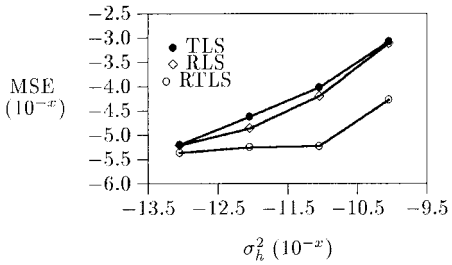

Fig. 2. MSE's of reconstructed images of the medium containing an off-center object under different σ_h^2 for a given $\sigma_n^2 = 8.99E{-}12$. Both axes are represented in terms of exponents.

the rod in a ring geometry, having a diameter of 8 cm (see [7]). The rod was located at either the center or an off-center location, with respect to the source/detector ring. The imaged region occupied an area of 10 cm $\times$ 10 cm enclosing the source/detector ring, and the area was discretized to 32×32 pixels. Therefore, in our simulation $m = 16^2$, $n = 32^2$. The absorption and scattering coefficients of the background medium were $\mu_a^b = 0.02$ cm^{-1} and $\mu_s^b = 10$ cm^{-1}. The scattering coefficient of the rod was the same as the background. The absorption coefficient distribution followed one positive cycle of the sinusoidal function, with the peak value being $\mu_a = 0.05$ cm^{-1}. Therefore the range of $\Delta\mu_a$ was between 0 and 0.03 cm^{-1}. In this work, we refer to a rod with such type of absorption coefficient distribution as a sine-like rod. The solution to the forward problem (generating $\mathbf{H}$ and $\mathbf{y}$) for the continuous wave case was obtained by analytically solving the diffusion equation using the normal mode series method described in Ref. [16]. To evaluate the effect of noise in the data and weight matrices, the matrix $\mathbf{H}$ was corrupted by additive white Gaussian noise with variance σ_h^2, while additive Gaussian noise with variance σ_n^2 was added to the observations.

As an objective metric we use the mean squares error (MSE) between the actual media properties and the reconstructed ones defined by

$$\mathrm{MSE} = \frac{1}{n}\|\mathbf{x} - \hat{\mathbf{x}}\|^2 \tag{5}$$

where n is the length of $\mathbf{x}$. To eliminate the potential bias because of a particular noise realization, we repeated each experiment for every noise level five times for different noise realizations. The MSE values reported below are the average of the MSE's resulting from five realizations.

For the off-center case, the data was corrupted by white Gaussian noise at different noise levels with variances $8.99E{-}14$, $8.99E{-}13$, $8.99E{-}12$, and $8.99E{-}11$, which correspond to 40 dB, 30 dB, 20 dB, and 10 dB signal-to-noise ratio (SNR), respectively.

Two sets of simulation experiments were performed for the off-center case. In the first, the noise variance added to $\mathbf{H}$ was fixed at $\sigma_h^2 = 8.99E{-}12$, while the additive noise variance for the data σ_n varied and took the following values: $8.99E{-}14$, $8.99E{-}13$, $8.99E{-}12$, and $8.99E{-}11$, which correspond to 40 dB, 30 dB, 20 dB and 10 dB SNR, respectively. In the second set of experiments, the additive noise for the data was fixed at $\sigma_n^2 = 8.99E{-}12$, while the noise in $\mathbf{H}$ were varied.

For each test medium and a given noise level, the proposed RQF-RTLS method was compared against the previously reported RLS [17] and RQF-TLS [7] methods, all using CG algorithms. Fig. 1 compares the MSE's obtained by different methods, when σ_n^2 is varied for a fixed value of σ_h^2. Fig. 2 shows the results when σ_h^2 is varied under a fixed σ_n^2. Fig. 3 shows the reconstructed images for $\sigma_n^2 = 8.99E{-}12$ and $\sigma_h^2 = 8.99E{-}12$, obtained by the RQF-TLS, RLS and RQF-RTLS methods, respectively.

For the center-rod case, the data were corrupted with white Gaussian noise with 20 dB SNR ($\sigma_n^2 = 1.79E{-}13$). The same amount of additive white Gaussian noise (same noise variance as in the data) was also added to $\mathbf{H}$. Results shown are averaged from five different noise realizations. Fig. 4 shows the reconstruction results for a noise realization by the RQF-TLS, RLS and RQF-RTLS methods, respectively. The regularization parameters in RLS and RQF-RTLS in both center and off-center cases are obtained by trial-and-error. Specifically, we first selected the regularization parameter by the Miller criterion in the RLS and then we increased or decreased the value by an order based on the MSE and the visual quality.

From the above simulation results, it is clear that RQF-RTLS yields more stable and accurate solutions than both the RLS and RQF-TLS approaches. The visual improvement is very significant. We also found that RLS outperforms RQF-TLS. This implies that the incorporation of an appropriate form of regularization into the LS formulation is more beneficial than considering the inaccuracies in the operator $\mathbf{H}$. Such results are not surprising: as has been shown in other studies, applying proper regularization in an inverse solver is extremely important and beneficial. However, to our knowledge, this work is the first report a successful application of RTLS for optical tomography problems.

IV. Summary and Conclusions

In this work, A RQF-RTLS approach was proposed for solving the linear inverse problem where the operator is nonconvolutional. The minimization of the modified RQF was accomplished with the CG method, which has potential computational advantages over the direct SVD method. We applied the RQF-RTLS approach to solve the perturbation equation in optical tomography. Simulation results confirmed that the RQF-RTLS is more robust to noise in the data and operator matrix than the RLS and RQF-TLS methods.

Note that for small size problems, as those simulated here, SVD can also be applied to the modified operator matrix $\mathbf{B}$ to yield the same RTLS solution. However, for larger size problems, the CG method should be more efficient. The investigation of such computational issues is one of future work. In our current studies, the regularization parameter was selected based on a trial-and-error process. The automation of the selection of the regularization parameter requires further investigation [18]. Another possible direction for future research is to use the relation between the MAP estimator and RQF-RTLS estimate developed in [19] in a manner similar to [10] for image restoration.

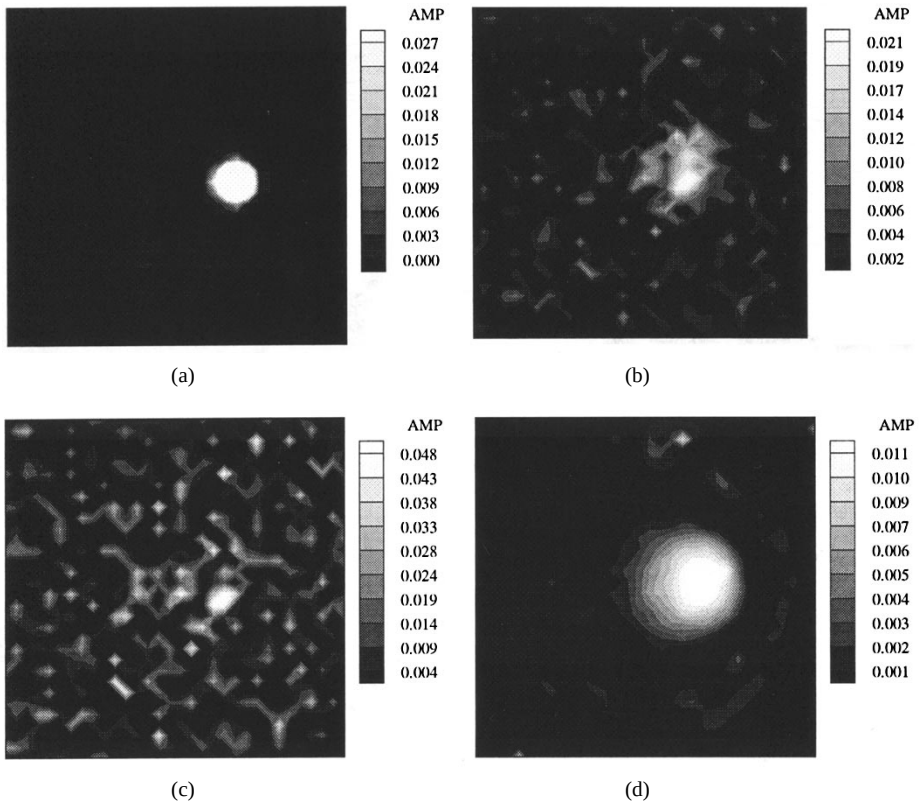

Fig. 3. Reconstruction results of a medium with an off-center rod with a sine-like distribution. The SNR of the data is 20 dB. The weights are corrupted by the same noise as in the data. The data size is 256×1. (a) Original image. (b) Reconstructed image using the RLS method. (c) Reconstructed image using the RQF-TLS method. (d) Reconstructed image using the RQF-RTLS method. All reconstruction results are obtained with 1000 iterations.

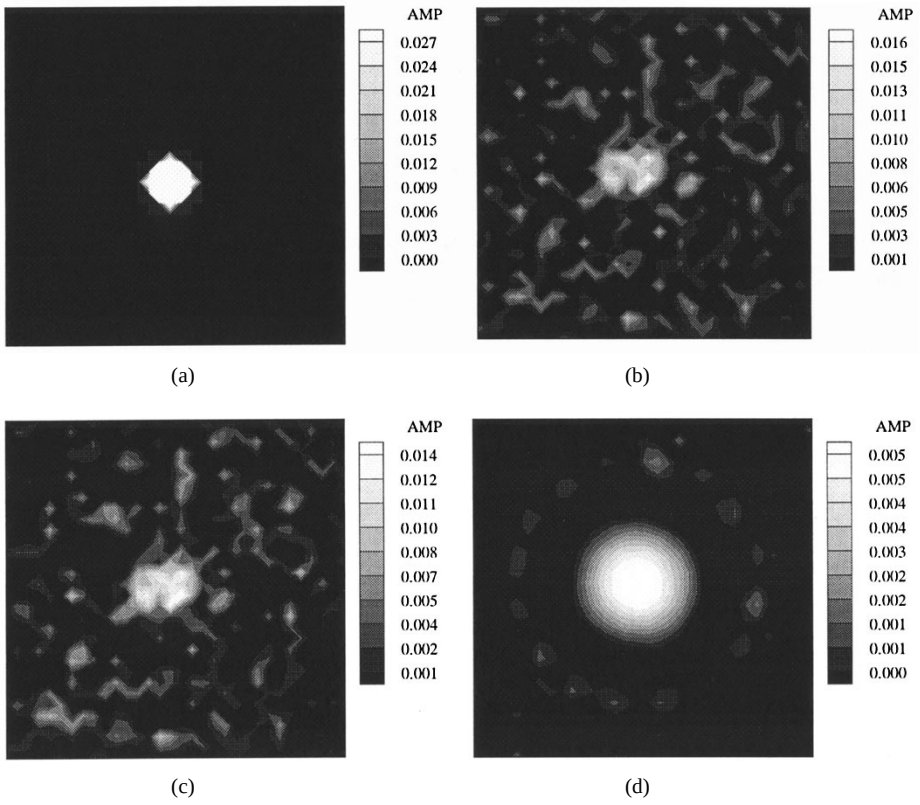

Fig. 4. Reconstruction results of a medium with a center rod with a sine-like distribution. The SNR of the data is 20 dB. The weights are corrupted by the same noise as in the data. The data size is 256×1. (a) Original image. (b) Reconstructed image using the RLS method. (c) Reconstructed image using the RQF-TLS method. (d) Reconstructed image using the RQF-RTLS method. All reconstruction results are obtained with 1000 iterations.

REFERENCES

[1] G. Demoment, "Image reconstruction and restoration: Overview of common estimation problems," *IEEE Trans Acoust., Speech, Signal Processing*, vol. 37, pp. 2024–2036, Dec. 1989.

[2] G. H. Golub and C. F. Van Loan, "An analysis of the total least squares problem," in *SIAM J. Numer. Anal.*, vol. 17, pp. 883–893, Dec. 1980.

[3] J. H. Justice and A. A. Vassiliou, "Diffraction tomography for geophysical monitoring of hydrocarbon reservoirs," *Proc. IEEE*, vol. 78, pp. 711–722, 1990.

[4] P. Li, S. W. Flax, E. S. Ebbini, and M. O'Donnell, "Blocked element compensation in phased array imaging," *IEEE Trans. Ultrason., Ferroelect., Freq. Contr.*, vol. 40, pp. 282–292, July 1993.

[5] G. H. Golub and C. F. Van Loan, *Matrix Computations*, 2nd ed. Baltimore, MD: John Hopkins Univ. Press, 1989.

[6] S. Van Huffel and J. Vandewalle, *The Total Least Squares Problem: Computational Aspects and Analysis*. Philadelphia, PA: SIAM, 1991.

[7] W. Zhu *et al.*, "A total least squares approach for the solution of the perturbation equation," in *J. Opt. Soc. Amer. A*, vol. 14, pp. 799–807, Apr. 1997.

[8] R. D. Fierro, G. H. Golub, P. C. Hansen, and D. P. O'Leary, "Regularization by truncated total least squares," *SIAM J. Sci. Comput.*, vol. 18, pp. 1223–1241, July 1997.

[9] V. Mesarović, N. P. Galatsanos, and A. K. Katsaggelos, "Regularized constrained total-least squares image restoration," *IEEE Trans. Image Processing*, vol. 4, pp. 1096–1108, Aug. 1995.

[10] V. Z. Mesarović, "Image restoration problems under point-spread function uncertainties," Ph.D. dissertation, Elect. Eng. Dept., Illinois Inst. Technol., Chicago, May 1997.

[11] X. Yang, T. K. Sarkar, and E. Arvas, "A survey of conjugate gradient algorithms for solution of extreme eigen-problem of a symmetric matrix," *IEEE Trans. Acoust., Speech, Signal Processing*, vol. 37, pp. 1550–1556, 1989.

[12] W. H. Press, S. A. Teukolsky, W. T. Vetterling, and B. P. Flannery, *Numerical Recipes in C: The Art of Scientific Computing*, 2nd ed. Cambridge, U.K.: Cambridge Univ. Press, 1992.

[13] W. Zhu, Y. Wang, N. P. Galatsanos, and J. Zhang, "Regularized total least squares reconstruction for optical tomographic imaging using conjugate Gradient Method," in *Proc. IEEE Int. Conf. Image Processing*, Santa Barbara, CA, Oct. 26–29, 1997, pp. 192–196.

[14] S. R. Arridge, "The forward and inverse problems in time resolved infra-red imaging," *SPIE Med. Opt. Tomogr.—Funct. Imag. Monitor.*, vol. IS11, pp. 35–64, 1993.

[15] R. L. Barbour, H. L. Graber, Y. Wang, J. Chang, and R. Aronson, "A perturbation approach for optical diffusion tomography using continuous-wave and time-resolved data," *SPIE Med. Opt. Tomogr.—Funct. Imag. Monitor.*, vol. IS11, pp. 87–120, 1993.

[16] Y. Q. Yao *et al.*, "Scattering characteristics of photon density waves from an object in a spherically two-layer medium," in *Proc. SPIE Conf. Optical Tomography, Photon Migration, and Spectroscopy of Tissue and Model Media*, San Jose, CA, Feb. 1995, vol. 2389, pp. 291–303.

[17] W. Zhu *et al.*, "A wavelet-based multiresolution regularized least squares reconstruction approach for optical tomography," *IEEE Trans. Med. Imag.*, vol. 16, pp. 210–217, 1997.

[18] G. H. Golub, M. Heath, and G. Wahba, "Generalized cross-validation as a method for choosing a good ridge parameter," *Technometrics*, vol. 21, pp. 215–223, 1979.

[19] W. Zhu, "Image reconstruction in optical tomography: Solution of the perturbation equation," Ph.D. dissertation, Dept. Elect. Eng., Polytech. Univ. Brooklyn, NY, June 1996.